Observation of Ultraviolet Rotational Band Contours of the DNA Base Adenine: Determination of the Transition Moment

Yonghoon Lee,[†] Michael Schmitt,[‡] Karl Kleinermanns,[‡] and Bongsoo Kim*[,§]

Department of Chemistry, KAIST, Daejeon 305-701, Korea, Advanced Photonics Research Institute, Gwangju Institute of Science and Technology, Gwangju 500-712, Korea, and Institut für Physikalische Chemie und Elektrochemie I, Heinrich Heine Universität, 40225 Düsseldorf, Germany

Received: June 21, 2006; In Final Form: August 27, 2006

We report the first observation and analysis of rotational band contours of the jet-cooled DNA base adenine for three vibronic bands at 36 062, 36 105, and 36 248 cm^{-1}. The lowest nπ^* and $\pi\pi^*$ states have been labeled with their excited-state vibronic symmetry, and a strong $\pi\pi^*-n\pi^*$ vibronic coupling via an out-of-plane vibrational mode has been revealed. The rotational band contours have been recorded by resonant two-photon ionization (R2PI) and analyzed by a genetic algorithm (GA) based fit to obtain the optimum band parameters. The vibronic band at 36 062 cm^{-1} shows dominant *c*-type character with transition dipole moment (TDM) components $\mu_a^2:\mu_b^2:\mu_c^2 = 0.09:0.17:0.74$ and those at 36 105 and 36 248 cm^{-1} show *abc*-hybrid character with predominantly in-plane TDM components. The band at 36 062 cm^{-1} has been assigned as the $n \rightarrow \pi^*$ transition, and the 36 105 cm^{-1} band as the $\pi \rightarrow \pi^*$ transition by the symmetry analysis. The band at 36 248 cm^{-1} provides evidence of the strong $\pi\pi^*-n\pi^*$ vibronic coupling via an out-of-plane vibrational mode.

I. Introduction

The nature of electronically excited states of the DNA and RNA bases determines their photophysical and photochemical properties. In view of the importance of UV absorption by DNA resulting in mutagenic and carcinogenic effects, much effort has been devoted to learn more about the electronically excited states of the nucleobases on a detailed molecular level.[1] Also, the excited-state study of clusters of these biological building blocks such as base pairs provides valuable information on hydrogen-bonding interactions as well as radiation-induced DNA damage pathways.[2] The R2PI and double resonance spectra of isolated adenine in a supersonic jet near 277 nm have been investigated by several groups.[3−7] The observed vibronic structure has been attributed either to transitions to excited $\pi\pi^*$ or nπ^* states or to mixed states thereof. All these experiments were done in low resolution and definite evidence to reveal the nature of the excited states is needed. Plützer and Kleinermanns tried to assign the vibronic states based on the rotational contour shapes of adenine, but the observed rotational contours could not be analyzed because of insufficient resolution.[7] Kim et al. assigned the bands at 36 062 and 36 105 cm^{-1} as an out-of-plane vibronic band of the $n \rightarrow \pi^*$ transition and the origin band of the $\pi \rightarrow \pi^*$ transition, respectively, based on dispersed fluorescence spectra.[8] The present work provides a new assignment of the three strong bands near the $\pi \rightarrow \pi^*$ origin based upon the high-resolution rotational band contour analysis of adenine. The rotational band contours resolved with 0.04 cm^{-1} UV bandwidth reveal their characteristic band types. The fit of the observed band contours yields TDM components, which enable us to assign their excited-state vibronic symmetries. Interestingly, two kinds of $n \rightarrow \pi^*$ transitions have been identified. One is a transition to a vibronic state of an in-plane vibrational mode (A′ symmetry) and the other is to an out-of-plane mode (A″ symmetry). Thus we obtained evidence for close-lying $\pi\pi^*$ and nπ^* states and their strong vibronic coupling within a narrow spectral window between 36062 and 36248 cm^{-1}.

II. Experiment

Details of the experimental setup for R2PI time-of-flight (TOF) mass spectroscopy have been published elsewhere.[9] Briefly, gas-phase adenine molecules were produced by heating a high-temperature pulsed nozzle that was a modified automobile fuel injection valve. By cooling the solenoid part with water, we could heat the pulsed nozzle to 600 °C. In this experiment adenine powder was heated to 270 °C, because adenine molecules decomposed at higher temperatures. The molecular beam was formed by expansion of a mixture of adenine vapor and Ar carrier gas through a pulsed nozzle into the vacuum. The pulsed jet was collimated by a 1.2 mm diameter skimmer at 7 cm from the nozzle. The molecular beam was then crossed by the frequency-doubled output of a dye laser (Lambda Physik Scanmate 2E) at 20 cm from the nozzle. The resulting ions were detected in a linear TOF mass spectrometer. A typical pressure was 3×10^{-5} Torr for the source chamber and 1×10^{-7} Torr for the detection chamber, while the pulsed nozzle was operated at 5 Hz with 160 Torr of Ar backing pressure, which provided the best signal-to-noise ratio for adenine ions. Figure 1 compares TOF mass spectra obtained at one-color R2PI by a UV laser tuned to the strongest vibronic band of adenine at 36105 cm^{-1} expanding with (a) 760 and (b) 160 Torr of Ar gas. At higher backing pressure the adenine−Ar mass peak (15.70 μs) was strongly enhanced and also the mass peak of adenine + 1 (12.67 μs) became stronger than that of bare adenine (12.63 μs). Probably, collision-induced processes such as cluster formation seemed to deplete the population of bare adenine at higher Ar backing pressure. Figure 2 compares low-

* To whom correspondence should be addressed. E-mail: bongsoo@kaist.ac.kr. Tel: +82-42-869-2836. Fax: +82-42-869-2810.
[†] Gwangju Institute of Science and Technology.
[‡] Heinrich Heine Universität.
[§] KAIST.

10.1021/jp063890z CCC: $33.50
Published on Web 10/05/2006

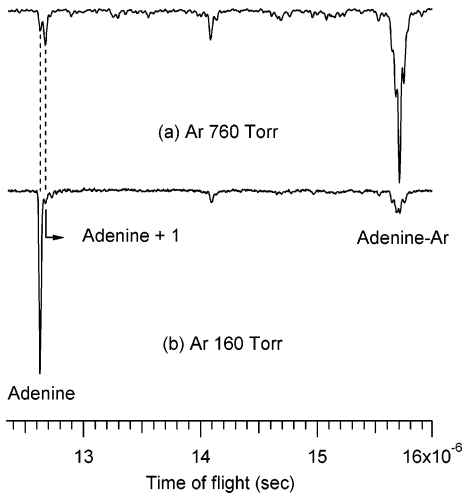

Figure 1. TOF mass spectra obtained by one-color R2PI expanding with (a) 760 and (b) 160 Torr of Ar. The excitation laser was tuned to the strongest transition of adenine at 36105 cm^{-1}.

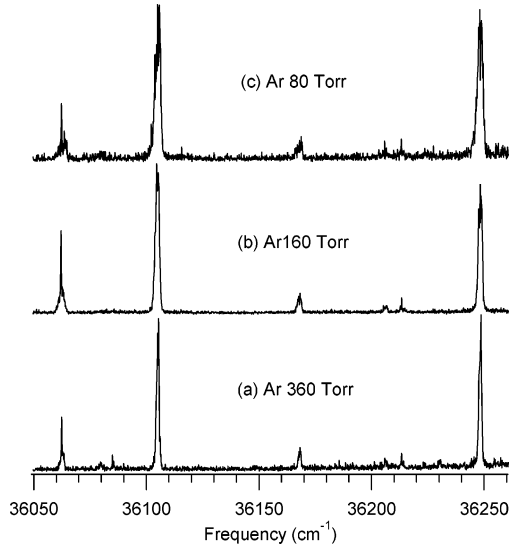

Figure 2. R2PI spectra of adenine obtained expanding with (a) 360, (b) 160, and (c) 80 Torr of Ar. The vertical scale of each spectrum was modified to compare signal-to-noise ratio.

resolution R2PI spectra of adenine obtained upon expanding with (a) 360, (b) 160, and (c) 80 Torr of Ar. When the backing pressure was decreased lower than 160 Torr, the signal-to-noise ratio was also decreased. The UV line width of the frequency-doubled dye laser was about 0.04 cm^{-1}, when an étalon was inserted in the oscillator cavity for high resolution scans. The fundamental line width was monitored simultaneously by an external monitor étalon (FSR = 0.25 cm^{-1}). A pulse energy of about 500 μJ/pulse was used to obtain the low resolution R2PI spectrum of adenine and about 360 μJ/pulse for the high resolution scans. To check if the absorption band was saturated in the case of high resolution contours, we took several spectra at laser powers of 1/2 and 1/4. When the ion signal decreased proportionally to the square of the laser power, we recorded the spectrum. Wavelength calibrations for high resolution scans were performed by simultaneously recording the LIF spectrum of I_2 within $\pm$0.006 cm^{-1}.[10]

III. Results and Discussion

Figure 3 shows the low resolution R2PI spectrum of adenine between 35 400 and 36 900 cm^{-1}. The UV bandwidth of the

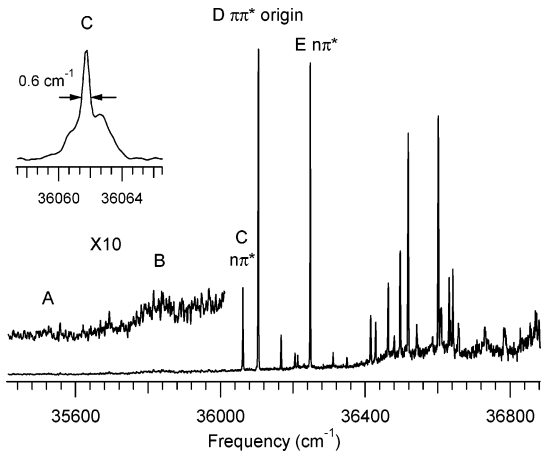

Figure 3. Low-resolution R2PI spectrum of adenine between 35 400 and 36 900 cm^{-1}. The inset shows the band shape of C band recorded in low resolution (0.24 cm^{-1}). The labeling of vibronic bands (A−E) is according to ref 3.

excitation laser is about 0.25 cm^{-1}. The strong vibronic bands at 36 062, 36 105, and 36 248 cm^{-1} are labeled as C, D, and E, respectively. The labeling is according to a previous report.[3] We could detect very weak signals between 35 400 and 36 050 cm^{-1}, which was labeled as A and B previously, without increasing the power or focusing the lasers.[3,7] Generally, the observed spectral features in the low resolution spectrum are in agreement with those reported previously by other groups.[3−7] Several sharp vibronic bands are observed within a narrow region followed by a diffuse and broad spectral feature. For the assignments of the excited states and the interpretation of the irregular vibronic structure in this narrow UV window, researchers have agreed that the strongest D band is the $\pi \rightarrow \pi^*$ origin, C and E bands belong to the same $n \rightarrow \pi^*$ transition, and the observed dense and irregular vibronic structure has been attributed to the strong vibronic coupling between the close-lying $\pi\pi^*$ and $n\pi^*$ states. The weak band observed at 35 503 cm^{-1} was assigned to the $n \rightarrow \pi^*$ origin by Kim et al.[3] Most of the observed vibronic structure is due to the 9H-tautomer, except some weak bands around 35 830 cm^{-1}, which are assigned to the 7H-tautomer using IR−UV double resonance spectroscopy.[7] Despite the reasonable interpretations of the observed vibronic structure of adenine, definite assignments of the close-lying $\pi\pi^*$ and $n\pi^*$ states and their vibronic coupling have not been reported yet.

Figure 4 shows high-resolution rotational contour spectra of the C, D, and E bands. Interestingly, the observed contour shapes of the C and E bands are very different, although they are thought to share the same upper electronic state, $n\pi^*$. First visual inspection of the gross shape of the contours in the low resolution spectrum (see the inset in Figure 3) already reveals a prominent Q-branch and therefore a predominant *c*-type of the C band. A genetic algorithm based fit[11] was used to obtain the optimum molecular parameters. The genetic algorithms based fitting strategy was recently improved[12] and used successfully for the automated assignment of very dense rovibronic spectra.[13] Even when no single line could be identified because of heavy overlapping of lines and large line widths, the absolute minimum of the cost function could be found by the GA, which were based on nature's principle to optimize qualities of individuals over many generations by reproduction, mutation, and selection of the most fittest ones. Therefore, the parameters that have to be fit are binary encoded and added to a string, which is called a chromosome. The quality of the individual solutions is evaluated using a weighted cross correlation of the

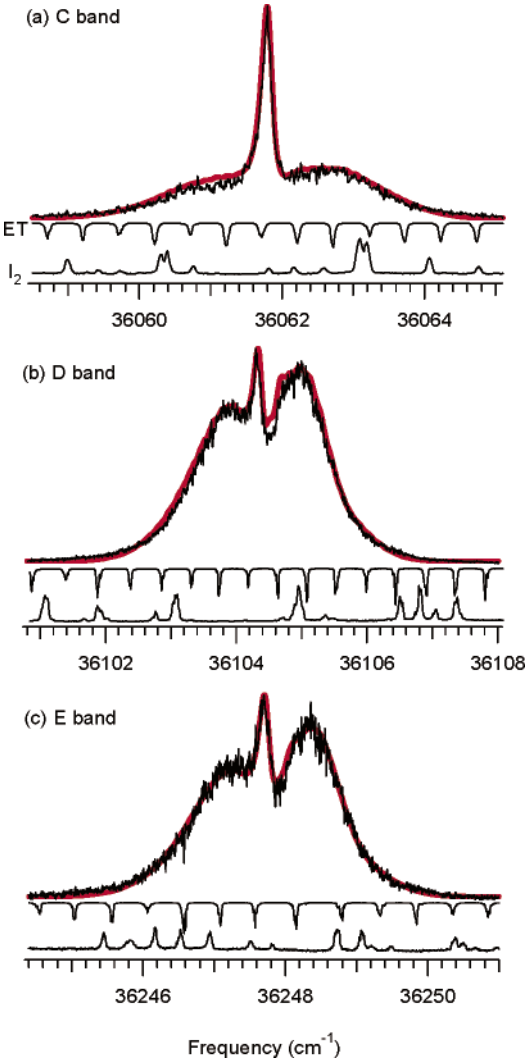

Figure 4. High-resolution rotational band contours (black) and their simulations (red) of the (a) C, (b) D, and (c) E bands of adenine. Each contour is shown together with the simultaneously recorded étalon fringe scan (ET) and I_2 LIF spectrum.

experimental and the simulated spectrum. Details of the GA fit can be found in ref 12. The microwave values determined by Brown et al.[14] were adopted for the ground-state rotational constants ($A'' = 2371.873(4)$, $B'' = 1573.3565(8)$, $C'' = 946.2576(4)$ MHz). We fit the changes of the rotational constants ($\Delta A = A' - A''$, $\Delta B = B' - B''$, and $\Delta C = C' - C''$) upon electronic excitation, the rotational temperature, the Lorentzian width of the spectral lines, and the spherical coordinate angles of the TDM vectors ϕ and θ in the molecular fixed frame. The angles determine the TDM components with respect to the inertial axes via the relations:

$$\mu_a = \mu \cdot \sin\phi \cos\theta$$

$$\mu_b = \mu \cdot \sin\phi \sin\theta$$

$$\mu_c = \mu \cdot \cos\phi$$

where μ is the absolute value of the TDM, θ is the angle between the projection of the TDM on the *ab*-plane and the *a*-axis, and ϕ is the angle between the TDM and the *c*-axis. The uncertainties of the parameters were estimated from five independent fits using different initial seeds in the GA procedure and are given in parentheses as a rough estimate of the reliability and the reproducibility of the fit. The fitted molecular parameters are

TABLE 1: Molecular Parameters of Adenine Obtained from a Fit to the Experimentally Observed Rotational Contours of C, D, and E Bands (Rotational Constants of the Ground State from Ref 14)

parameters	C band	D band	E band
ΔA (MHz)	50(50)	2(20)	−2(20)
ΔB (MHz)	−90(150)	−43(10)	−32(10)
ΔC (MHz)	−1(50)	−20(10)	−26(10)
ϕ (deg)	31(2)	64(2)	63(2)
θ (deg)	54(2)	62(2)	55(2)
$\mu_a^2:\mu_b^2:\mu_c^2$ [a]	0.09:0.17:0.74	0.18:0.63:0.19	0.26:0.53:0.21
ν_0 (cm^{-1})	36061.8	36104.3	36247.7
Δ_{Gauss} (MHz)[b]	1800	1200	1500
$\Delta_{Lorentz}$ (MHz)	3100(200)	3100(200)	3500(400)
T_{rot} (K)	6.1(5)	4.9(2)	5.3(2)

[a] Calculated from the spherical coordinates ϕ and θ. See text for details. [b] Fixed in the fit to the values determined from a simultaneously taken étalon scan.

listed in Table 1. From the TDM components of the C, D, and E bands, $\mu_a^2:\mu_b^2:\mu_c^2 = 0.09:0.17:0.74$, 0.18:0.63:0.19, and 0.26:0.53:0.21, respectively, it is found that the TDM for the C band is mainly polarized along the *c*-axis perpendicular to the *ab*-plane, and those for D and E bands are polarized mainly in the *ab*-plane but show some *c*-type character. When we tried to limit the TDM orientation for these two bands purely in plane ($\phi = 90°$), as expected for a $\pi \rightarrow \pi^*$ transition of a planar molecule, the results of the fits with this constraint were of considerably lower quality than those given in Table 1. This fact points to a considerable mixing of the nπ^* and the $\pi\pi^*$ states, as was predicted by Marian.[15] In this case, the lack of symmetry for the excited states facilitates the vibronic coupling and explains the rather large intensity of the n $\rightarrow \pi^*$ transition by intensity borrowing.

Adenine in its electronic ground state is a planar molecule, as can be inferred from the small inertial defect, calculated from the microwave rotational constants (cf. Table 1). If the geometry distortions of adenine in its electronically excited states are small, we can use approximate selection rules for its vibronic transitions. When we assume the C_s point group (planar geometry of adenine in all states), the vibronic symmetries of the states responsible for the C, D, and E bands are determined by the selection rule for vibronic transitions:

$$\Gamma^{f}_{elec} \otimes \Gamma^{f}_{vib} \otimes \Gamma_{TDM} \otimes \Gamma^{i}_{elec} \otimes \Gamma^{i}_{vib} \supseteq A'$$

Because the ground vibronic state (initial state) is totally symmetric (A′), the final vibronic state should have A′ symmetry for an in-plane polarized TDM (A′), and A″ symmetry for a TDM polarized along the *c*-axis (A″).

Because the D band was assigned to the $\pi \rightarrow \pi^*$ origin by the previous investigations, and the TDM is in-plane polarized, vibronic symmetry of the upper state of D band is assigned to $\Gamma_{elec}(A') \otimes \Gamma_{vib}(A')$. Plützer and Kleinermanns showed that the C and E bands had the same spectral isotopic shift pattern for the two amino deuterated (NHD and NDH), the N9H deuterated, and the CH deuterated species, whereas the D band had a different isotopic pattern.[7] They observed that the spectral shifts depended on the differences of zero-point energies in the ground and excited state and concluded that the C and E bands shared the same electronically excited state, nπ^*. Considering the nπ^* state has A″ symmetry and $\Gamma_{TDM} = A''$, the symmetry of the upper vibronic state of the C band is assigned to $\Gamma_{elec}(A'') \otimes \Gamma_{vib}(A')$. Despite sharing the same upper electronic state with the C band, the TDM orientation of the E band is polarized in the *ab*-plane, as that of the D band. Most of the previous studies

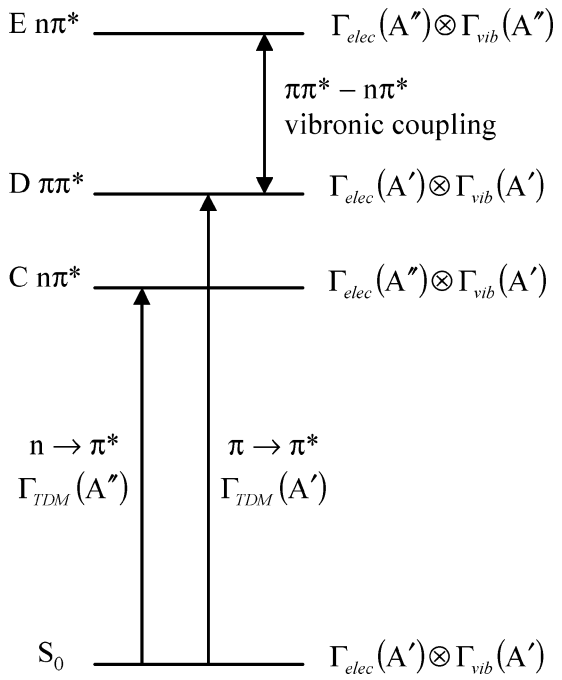

Figure 5. Summary of the symmetries of vibronic transitions corresponding to the C, D, and E bands.

attribute the rather dense and irregular vibronic structure observed on the blue side of the D band to out-of-plane vibrational modes of the nπ* state due to strong vibronic coupling between $\pi\pi$* and nπ* states. This interpretation is clearly confirmed by the observation of a predominantly in-plane polarized TDM for the E band. The intensity borrowing of the E band is rationalized by the strong $\pi\pi$*−nπ* vibronic coupling via out-of-plane vibrational modes. The vibronic symmetry of the excited state of the E band should become $\Gamma_{elec}(A'') \otimes \Gamma_{vib}(A'')$, because the upper electronic state of the E band is nπ* and the TDM is in-plane polarized (A′). The out-of-plane A″ vibrational mode mediates the intensity borrowing of the E band from the D band. The excitation of A″ vibrational modes in the nπ* state is forbidden, if vibronic mixing is negligible. When a forbidden transition occurs by means of vibronic coupling, the band structure is entirely determined by the vibronic species of the upper and lower states.[16] Therefore, the observed band contour of the E band looks very similar to that of the D band. The spectral intensities of the D and the E bands are similar, which also points to strong mixing of the $\pi\pi$* and nπ* states. Consequently, we could identify two different kinds of n → π* transitions. One is the normal n → π* transition to an A′ vibrational mode and the other is the n → π* transition to an A″ vibrational mode induced by strong vibronic coupling to the $\pi\pi$* state. The transition schemes of the C, D, and E bands are summarized in Figure 5.

The inertial defect of adenine in its electronic ground states calculated from the MW rotational constants[14] amounts to −0.2 amu·Å^2, showing the planarity of the structure of ground state. According to the ab initio study of 9H-adenine reported by Perun et al.,[17] the equilibrium geometry of the S_0 and $^1\pi\pi$* states are almost planar. The nonplanarity is confined to a slight pyramidalization of the amino group in both states. For the ^{1}nπ* state, a significant out-of-plane deformation of six-membered ring was predicted by calculation. The in-plane components of the TDM in the rotational contour of the C band may be due to this out-of-plane distortion of the chromophore.

A slightly different result for the excited-state geometries has been found by Marian using time dependent DFT calculations.[15] The minimum energy geometry for the ^{1}nπ* state is found to be planar for the ring system, whereas the amino group is pyramidal. For the lowest $^1\pi\pi$* state a strong puckering of the six-membered ring is found. It is found that this state is strongly mixed with the ^{1}nπ* state. If the excited states of adenine were nonplanar, the ^{1}nπ* state could borrow its intensity directly from the $^1\pi\pi$* state; thus the unexpectedly high intensity of the C band can be explained. By taking the geometry of the ground state, the ^{1}nπ* state and the $^1\pi\pi$* state from ref 15, we calculated the changes of the rotational constants for the transition $\pi\pi$* ← S_0 to be −9, −45, and −18 MHz, and those for the transition nπ* ← S_0 are −28, −25, and −13 MHz. These values are close to the experimentally determined changes of the rotational constants, given in Table 1. The orientation of the TDM of the optimized ^{1}nπ* state from ref 15 gives a band type of 6% *a*-, 4% *b*- and 90% *c*-type, close to the experimentally determined values for the C-band given in Table 1. The $^1\pi\pi$* state, which is observed in our experiment as D-band, has to be compared to the adiabatically lowest state from ref 15. The $^1\pi\pi$* ← S_0 transition has mainly LUMO ← HOMO character and shows nearly equal amounts of *a*- and *b*-type, with some *c*-type contribution from the mixing of the ^{1}nπ* state. Theoretically determined values predict that the D-band would have similar *a*- and *b*-type character.[18]

Hochstrasser and Marzzacco[19] and Andréasson et al.[20] suggested that coupling of $\pi\pi$* and nπ* states is responsible for the fluorescence quenching of the $\pi\pi$* states of the DNA bases and other heterocyclic compounds. Lim showed the effect of vibronic coupling between nearby $\pi\pi$* and nπ* states on the radiationless transition rate.[21] In his model the out-of-plane vibration that couples the $\pi\pi$* and nπ* states acts as an efficient acceptor mode for the radiationless decay to the ground state.

IV. Conclusions

We report the first observation and analysis of UV rotational band contours of the vibronic transitions of adenine. From the analysis we assigned the close-lying $\pi\pi$* and nπ* states and their strong vibronic coupling via out-of-plane vibrational modes based on the assumption of a planar geometry of a purine chromophore. Two kinds of n → π* transitions are identified. One is the transition to an in-plane vibrational mode (A′) and the other is the transition to an out-of-plane vibrational mode (A″) which mediates the $\pi\pi$* − nπ* vibronic coupling. Usually the oscillator strength of the n → π* transition is estimated to 1 or 2 orders-of-magnitude smaller than that of the π → π* transition. The intensity of the n → π* transition can be borrowed from the π → π* transition through vibronic mixing. More experimental and theoretical works are required to understand the excited states of adenine in detail. Unfortunately, higher resolution experimental studies using a single mode ring dye laser or a pulse amplified ring dye laser may not be feasible due to the very short excited-state lifetime[5,22−27] of adenine, although the information of detailed excited−state geometries of $\pi\pi$* and nπ* states would be invaluable. Application of MATI (or ZEKE) spectroscopy to adenine by a (1+1′) two-photon scheme via the C, D, E, and other bands are encouraged to elucidate Franck−Condon factors and selection rules involved in both S_0 → $\pi\pi$*/nπ* and $\pi\pi$*/nπ* → $D_0(\pi^{-1})/D_1(n^{-1})$ transitions.

Acknowledgment. We thank W. Leo Meerts for providing the genetic algorithm program, C. M. Marian for providing the optimized geometries and TDM orientations of adenine, and Profs. S. K. Kim and E. C. Lim for valuable discussions. B.K.

is thankful for the financial support from KRF through ABRL (R14-2005-033-0100) and KOSEF through the Center for Intelligent Nano-Bio Materials (R11-2005-008-00000-0). M.S. and K.K. thank the DFG (SFB 663, TP2 and 4) for financial support.

References and Notes

(1) Crespo-Hernández, C. E.; Cohen, B.; Hare, P. M.; Kohler, B. *Chem. Rev.* **2004**, *104*, 1977 and references therein.

(2) Nir, E.; Kleinermanns, K.; de Vries, M. S. *Nature* **2000**, *408*, 949.

(3) Kim, N. J.; Jeong, G.; Kim, Y. S.; Sung, J.; Kim, S. K. *J. Chem. Phys.* **2000**, *113*, 10051.

(4) Nir, E.; Kleinermanns, K.; Grace, L.; de Vries, M. S. *J. Phys. Chem. A* **2001**, *105*, 5106.

(5) Lührs, D. C.; Viallon, J.; Fischer, I. *Phys. Chem. Chem. Phys.* **2001**, *3*, 1827.

(6) Plützer, Chr.; Nir, E.; de Vries, M. S.; Kleinermanns, K. *Phys. Chem. Chem. Phys.* **2001**, *3*, 5466.

(7) Plützer, Chr.; Kleinermanns, K. *Phys. Chem. Chem. Phys.* **2002**, *4*, 4877.

(8) Kim, N. J.; Kang, H.; Park, Y. D.; Kim, S. K. *Phys. Chem. Chem. Phys.* **2004**, *6*, 2802.

(9) Lee, Y.; Yoon, Y.; Baek, S. J.; Joo, D.-L.; Ryu, J.-S.; Kim, B. *J. Chem. Phys.* **2000**, *113*, 2116.

(10) Gerstenkorn, S.; Luc, P. *Atlas du Spectre d'Absorption de la Molécule d'Iode Entre 14800−20000 cm*$^{-1}$; CNRS: Paris, 1978.

(11) Hageman, J. A.; Wehrens, R.; de Gelder, R.; Meerts, W. L.; Buydens, L. M. C. *J. Chem. Phys.* **2000**, *113*, 7955.

(12) Meerts, W. L.; Schmitt, M.; Groenenboom, G. *Can. J. Chem.* **2003**, *82*, 804.

(13) Schmitt, M.; Ratzer, Ch.; Kleinermanns, K.; Meerts, W. L. *Mol. Phys.* **2004**, *102*, 1605.

(14) Brown, R. D.; Godfrey, P. D.; McNaughton, D.; Pierlot, A. P. *Chem. Phys. Lett.* **1989**, *156*, 61.

(15) Marian, C. M.; *J. Chem. Phys.* **2005**, *122*, 104314.

(16) Herzberg, G. In *Molecular Spectra and Molecular Structure*; Reprint of 2nd ed.; Krieger: Malabar, 1991; Vol. 3, p 241.

(17) Perun, S.; Sobolewski, A. L.; Domcke, W. *J. Am. Chem. Soc.* **2005**, *127*, 6257.

(18) Private communication with C. M. Marian.

(19) Hochstrasser, R. M.; Marzzacco, C. *J. Chem. Phys.* **1968**, *49*, 971.

(20) Andréasson, J.; Holmén, A. Albinsson, B. *J. Phys. Chem. B* **1999**, *103*, 9782.

(21) Lim, E. C. *J. Phys. Chem.* **1986**, *90*, 6770.

(22) Kang, H.; Lee, K. T.; Jung, B.; Ko, Y. J.; Kim, S. K. *J. Am. Chem. Soc.* **2002**, *124*, 12958.

(23) Ullrich, S.; Schultz, T.; Zgierski, M. Z.; Stolow, A. *J. Am. Chem. Soc.* **2004**, *126*, 2262.

(24) Kang, H.; Jung, B.; Kim, S. K. *J. Chem. Phys.* **2003**, *118*, 6717.

(25) Canuel, C.; Mons, M.; Piuzzi, F.; Tardivel, B.; Dimicoli, I.; Elhanine, M. *J. Chem. Phys.* **2005**, *122*, 074316.

(26) Ritze, H.-H.; Lippert, H.; Samoylova, E.; Smith, V. R.; Hertel, I. V.; Radloff, W.; Schultz, T. *J. Chem. Phys.* **2005**, *122*, 224320.

(27) Cohen, B.; Hare, P. M.; Kohler, B. *J. Am. Chem. Soc.* **2003**, *125*, 13594.